Computers and Concrete, *Vol. 16, No. 6 (2015) 881-896*
DOI: http://dx.doi.org/10.12989/cac.2015.16.6.881

Experimental crack analyses of concrete-like CSCBD specimens using a higher order DDM

Hadi Haeri*

Department of Mining Engineering, Bafgh Branch, Islamic Azad University, Bafgh, Iran

(Received November 14, 2015, Revised December 7, 2015, Accepted December 9, 2015)

Abstract. A simultaneous analytical, experimental and numerical analysis of crack initiation, propagation and breaking process of the Central Straight through Crack Brazilian Disk (CSCBD) specimens under diametrical compression is carried out. Brazilian disc tests are being accomplished to evaluate the fracturing process based on stress intensity factors (SIFs). The effects of crack inclination angle and crack length on the fracturing processes have been investigated. The same experimental specimens have been numerically modeled by a higher order indirect boundary element method (HDDM). These numerical results are compared with the existing experimental results proving the accuracy and validity of the proposed numerical method.

Keywords: concrete-like specimens; CSCBD; SIFs; DDM; higher order elements

1. Introduction

Wing and secondary cracks play a vital role in the propagating process of the pre-existing cracks in brittle materials under compression. Practically, in classic fracture mechanics, three types of loading modes were proposed to study the crack propagation in the pre-cracked solid materials i.e., i) Mode I (tension or opening Mode) ii) Mode II (in-plane shearing Mode) and Mode III (tearing or out of plane shearing Mode). The pre-existing cracks in concrete-like brittle solids (or natural rocks) are normally under compressive loading rather than under tension, shear or mixed mode loadings (Ke *et al*. 2008).

In the crack propagation process of pre-cracked concrete specimens, new cracks (i.e., wing cracks and secondary cracks) may be observed which are emanating from the original tips of pre-existing cracks. These propagating wing cracks follow in the direction (approximately) parallel to the maximum compressive loading direction and sometimes coalescing with other propagating and/or pre-existing cracks (Hoek and Bieniawski 1965, Lee and Jeon 2011). However, wing cracks are usually produced due to tension while secondary cracks may initiate due to shear. Initiation and propagation of wing cracks in concrete specimens (brittle solids) is favored relative to the secondary cracks (because of the lower tensile toughness of these materials compared to that of shear (Bieniawski 1967).

*Corresponding author, E-mail: haerihadi@gmail.com

http://www.techno-press.org/?journal=cac&subpage=8 ISSN: 1598-8198 (Print), 1598-818X (Online)

Many researches have been devoted to study the crack initiation, crack propagation and coalescence of the pre-existing cracks in pre-cracked specimens of various brittle materials, including concrete or rock-like brittle materials under compressive loading (Ravi-Chandar and Knauss 1984, Ingraffea 1985, Shen *et al*. 1995, Yang *et al*. 2009, Park and Bobet 2010, Janeiro and Einstein 2010, Yang 2011, Cheng-zhi and Ping 2012, Wallin 2013).

Brazilian disc tests may be regarded as some of the most suitable tests for investigating the mixed mode (Mode I and Mode II) fracturing and evaluating the static and dynamic fracture toughness for rocks and concrete-like specimens containing central pre-existing cracks (flaws) or discontinuities. The fracturing processes and cracks coalescence of brittle materials such as rocks or concrete-like specimens under compressive line loadings may also be studied by these tests (Ayatollahi and Aliha 2008, Wang 2010, Dai *et al*. 2010, 2011, Ayatollahi and Sistaninia 2011, Wang *et al*. 2011. 2012, Haeri 2015a, b, c). Due to low tensile strength of rocks and concrete like materials, the crack initiation and fracturing process of the Brazilian disc specimens often happen very soon under compressive line loading. Al-Shayea (2005) studied the crack propagation paths in the Central Straight through Crack Brazilian Disk (CSCBD) specimens of brittle limestone considering different crack inclination angles under mixed mode I/II loading. The influence of confining pressure and temperature on the crack initiation and propagation of the rock samples is also considered in his analysis and finally his experimental results were compared with theoretical predictions of crack initiation angles.

In addition, the indirect Boundary Element Method (BEM) is used to simulate the fracturing process of brittle materials (Crouch 1967, Haeri 2015a). It has also been shown that these numerical results are in good agreement with their corresponding experimental results. The HDDM2D code (a version of indirect BEM known as displacement discontinuity method (DDM) using higher displacement discontinuity and special crack tip elements) is employed for predicting the wing cracks initiation. In this computer code (iterative method code), a set of complex mathematical equations relevant to the stress intensity factor SIFs and fracture toughness are also applied to properly simulate the experimental tests.

In this study, the HDDM2D code is selected as a numerical modeling device to simulate the crack initiation, propagation and fracturing paths of CSCBD concrete-like specimens under compressive line loading**.** Therefore, several Brazilian tests on CSCBD specimens of concrete-like materials containing central straight through cracks with different crack lengths in the central part of the specimens are performed to analyze the crack propagation and fracturing process of brittle materials. The CSCBD specimens (which are specially prepared from PCC, fine sands and water) containing central straight through cracks of different lengths and different pre-existing crack inclination angles were being tested under compressive line loading in a concrete laboratory. Then, these experimental works are also simulated numerically by a modified higher order displacement discontinuity method and the crack propagation are studied based on the Mode I and Mode II stress intensity factors (SIFs) using the LEFM principles (Irwin G R 1957). These fracturing analysis get completed by comparing the numerical results with the experimental results which in turn demonstrates the accuracy and effectiveness of the proposed numerical method.

2. Stress intensity factors (SIFs) for CSCBD specimens

Consider a Central Straight Through Crack Brazilian Disk (CSCBD) specimen with radius, R containing a central straight through crack with a half-length, b and inclination angle, ψ, changing

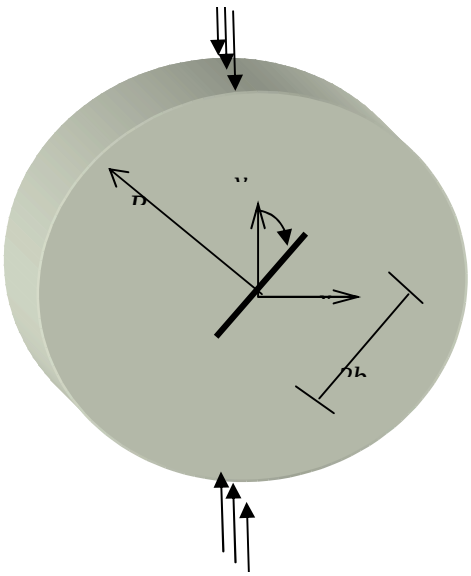

Fig. 1 A typical CSCBD specimen containing a center slant crack

counterclockwise from the *y* axis, and the line load, *F* is acting parallel to the *y* axis (as shown in Fig. 1). The analytical solution of this typical fracture mechanics problem is given in the literature (Atkinson *et al*. 1982, Whittaker *et al*. 1992). Based on Fig. 1, the analytical solution for Mode I and Mode II stress intensity factors (SIFs) in a CSCBD specimen can be estimated from

$$K_I = \frac{F\sqrt{b}}{\sqrt{\pi}RB}\omega_I, \qquad K_{II} = \frac{F\sqrt{b}}{\sqrt{\pi}RB}\omega_{II} \tag{1}$$

where, K_I and K_{II} are Mode I and Mode II stress intensity factors (SIFs), respectively expressed in MPa m1/2, F is the compressive load at breakage in Newton, B is thickness (length) of the disk in mm, and ϖ_I and ϖ_{II} are the non-dimensional coefficients depending on the crack inclination angle, ψ, which can be defined as

$$\begin{aligned} \omega_I &= 1 - 4\sin^2\psi + 4\sin^2\psi(1 - 4\cos^2\psi)(\frac{b}{R})^2 \\ \omega_{II} &= [2 + (8\cos^2\psi - 5)(\frac{b}{R})^2]\sin 2\psi \end{aligned} \tag{2}$$

As it can be seen in Eqs. (1) and (2), the SIFs of crack tips are affected by the crack geometry such as half crack length (b), radius (R), thickness (B) and crack inclination angle (ψ).

In analytical solution, thickness (B) of the disk is essential to estimate the value of SIFs. The value of thickness is assumed to be 30 mm.

Variations of ϖ_I and ϖ_{II} for the assumed CSCBD specimen with a constant b/R ratio equal to 0.3 are illustrated in Fig. 2 considering different ψ angles.

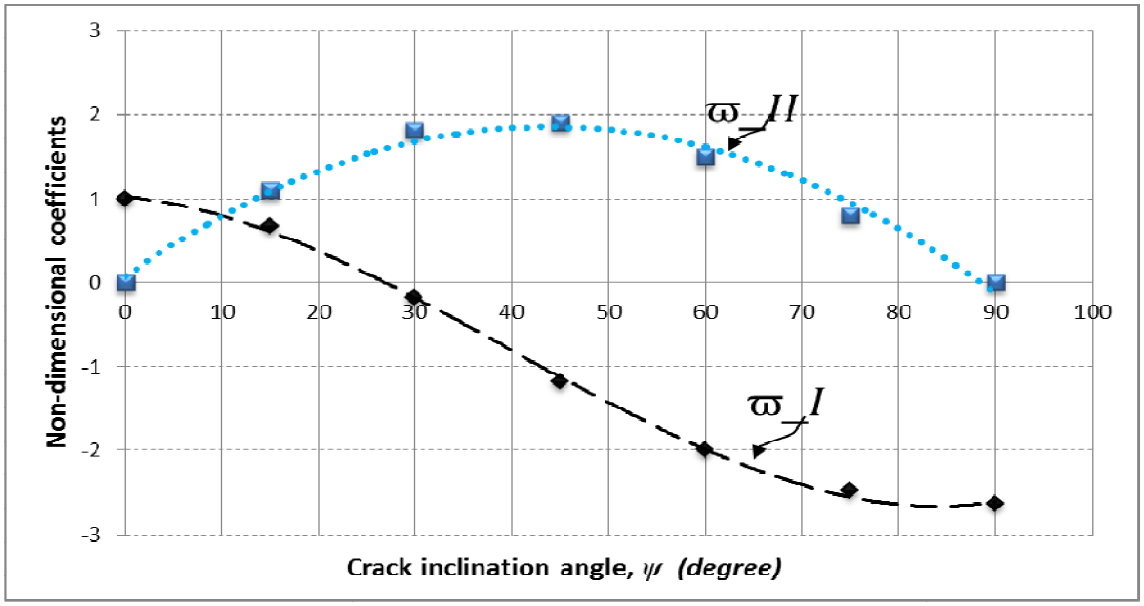

Fig. 2 Variation of ϖ_I and ϖ_{II} with crack inclination angles for a CSCBD specimen

As shown in this figure, ϖ_I decreases monotonically with increasing ψ angle, while ϖ_{II} has a global maximum value at ψ=45° (ϖ_{II} =1.91). Furthermore, Fig. 2 implies that pure Mode I loading is achieved only at ψ=0°(ϖ_I =1), whereas pure Mode II loading is obtained at ψ=27-30° (ϖ_{II} =1.7-1.8). However, in this case, the crack is not under tension-shear deformation but is under compression/shear deformation.

3. Experimental studies

Some specially prepared CSCBD specimens (from concrete-like brittle substances) are being tested in a concrete laboratory to study the crack propagation process of the pre-cracked brittle solids such as concrete specimens.

3.1 CSCBD specimen preparation and its mechanical properties

The CSCBD specimens of concrete-like materials with 100 mm, diameters and 30 mm, thickness are specially prepared from a mixture of Portland Pozzolana cement (PPC), fine sands and water. Table 1 gives the ingredient ratios (%) and mechanical properties of the prepared concrete-like specimens tested in the concrete laboratory before inserting the cracks.

The tensile strength (σ_t) for a typical crack free (intact) concrete-like specimen is

$$\sigma_t = \frac{2F}{\pi BR} \tag{3}$$

where F is the applied compressive load in KN, B is thickness of the disc specimen, and R is radius of the disc specimen.

Table 1 Ingredient ratios (%) and mechanical properties of the concrete-like specimens

Ingredients ratio (%)			Mechanical properties				
PP.cement	Fine sands	water	Tensile strength (MPa)	Uniaxial compression strength (MPa)	Fracture toughness (MPa m1/2)	modulus of elasticity (GPa)	Poisson's ratio
44.5	22.5	33	3.81	28	0.3	17	0.21

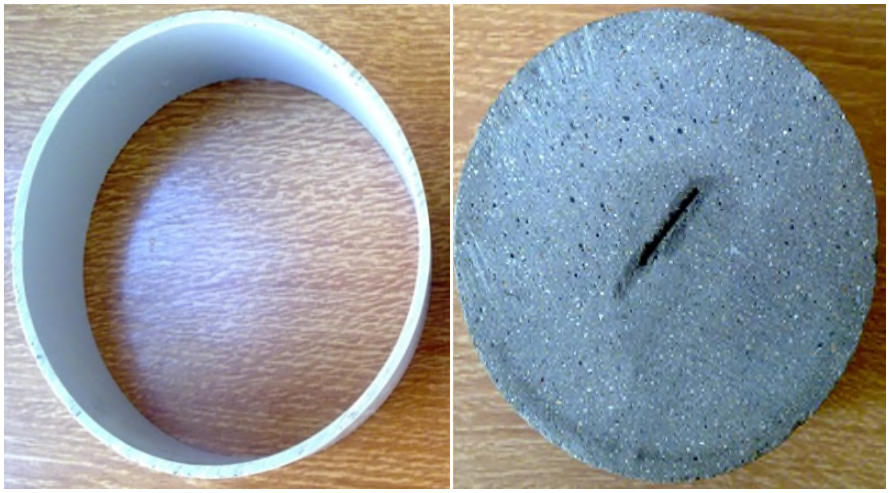

Fig. 3 A typical concrete-like Brazilian disc specimen

Various Brazilian tests were conducted on concrete-like CSCBD specimens (each specimen contains a central straight through crack). These cracks were created by inserting thin metal shims with 10, 20, 30, 40, 50 mm width and 1 mm thickness into the specimens (during the specimens casting in the mold) as shown in Fig. 3.

Several CSCBD specimens of concrete-like materials (with the same crack geometry) were prepared and tested in the laboratory. The CSCBD specimens containing two cracks of different inclination angles are also prepared and tested. A digital load-controlled testing machine with a capacity of 100 KN is used to test the pre-cracked concrete-like disc specimens. The disc Brazilian test (Indirect tensile testing of concrete known as the Brazilian Test) includes loading a cylindrical specimen with compressive line loads which act parallel to and along the vertical diametrical plane. The compressive line loading, F was diametrically applied and the loading rate was kept at 0.5MPa/s during the tests.

In this research, three specimens were prepared for each experimental test and as a whole, thirty six CSCBD specimens (Brazilian discs with different crack lengths and two crack inclination angles, ψ=45° and ψ=75°) were prepared and tested.

3.2 Fracturing mechanism of CSCBD specimens observed by experimental tests

The concrete-like CSCBD specimens were tested experimentally and the results were used to analyze the breaking loads and the crack propagation process of the pre-cracked disc specimens.

The crack propagation process of the CSCBD specimens are discussed considering the two

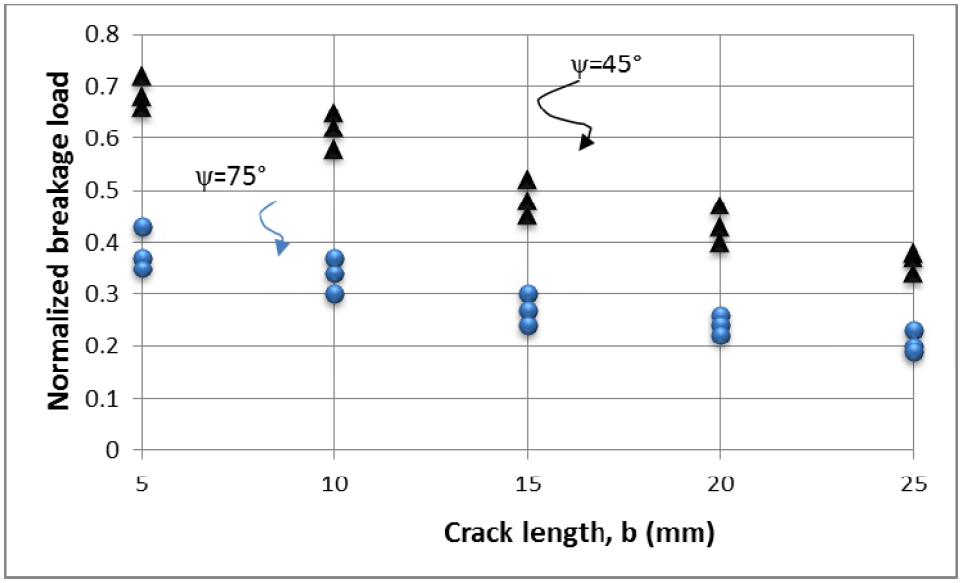

Fig. 4 Normalized breaking load versus crack length for two cases, ψ=45° and ψ=75°

cases of disc specimens with: i) crack inclination angle, ψ=45° and ii) crack inclination angle, ψ=75°.

3.2.1 Fracturing mechanism of CSCBD specimens

It is obvious that the pre-cracked concrete-like disc specimens have a lower strength compared to the un-cracked specimens (specimens having no cracks). The analysis of breaking load of the pre-cracked disc specimens containing a central straight through crack (or CSCBD) with two orientations is of paramount importance to study the behavior of the brittle materials. Fig. 4 describes the variation of the normalized breaking load for CSCBD specimens. The breaking load of the CSCBD specimens is normalized by the average breaking load of the un-cracked specimens. It should be noted that the average breaking load of un-cracked specimens is about 18 KN.

The normalized breaking loads for the CSCBD specimens are usually less than one because the pre-existing crack decreases the final strength of specimen (Fig. 4). In the CSCBD specimens, the normalized breakage loads decreases monotonically with increasing crack lengths, b (for both inclination angles, ψ =45° and ψ =75°).

3.3 Analyzing the crack propagation mechanism of CSBDC specimens

Experimental tests carried out on the pre-cracked concrete-like specimens considering the two cases: i) CSBDC specimens with crack inclination angle, ψ =45° and ii) CSBDC specimens with crack inclination angle, ψ =75°.

In this research, the mechanism of crack initiation and crack propagation emanating from the cracks already exist in CSBDC specimens (containing two different crack inclination angles; ψ=45° and 75°) is experimentally investigated. Figs. 5 and 6(a)-(f) illustrate the propagating mechanism of single cracked disc specimens which are propagating in form of wing cracks spreading in a curved path and continue their growth in a direction (approximately) parallel to the

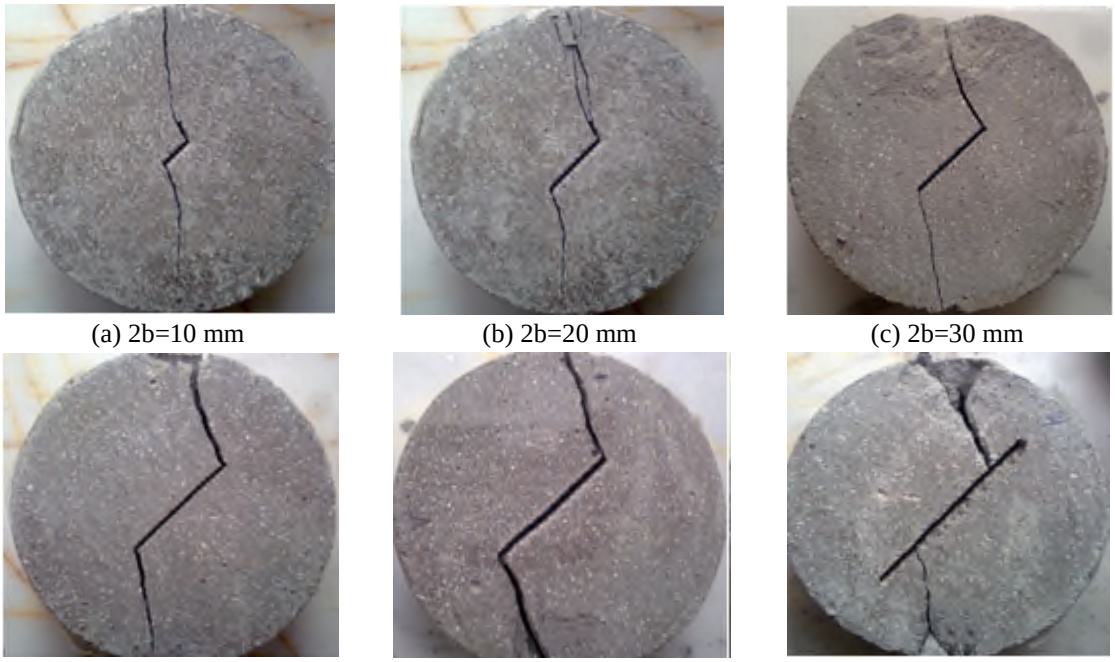

(a) 2b=10 mm (b) 2b=20 mm (c) 2b=30 mm

(d) 2b=40 mm (e) 2b=50 mm (f) 2b=60 mm

Fig. 5 Cracking patterns in CSCBD specimens with different crack lengths for: ψ=45°; (a) 2b=10 mm; (b) 2b=20 mm; (c) 2b=30 mm; (d) 2b=40 mm; (e) 2b=50 mm; (f) 2b=60 mm

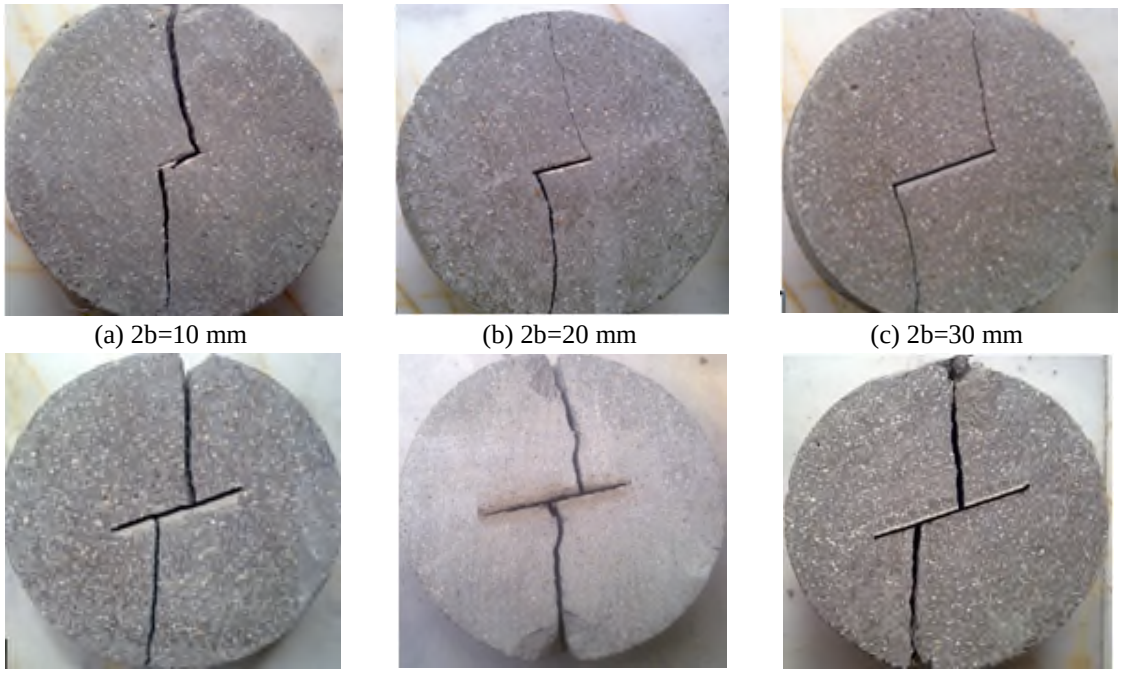

(a) 2b=10 mm (b) 2b=20 mm (c) 2b=30 mm

(d) 2b=40 mm (e) 2b=50 mm (f) 2b=60 mm

Fig. 6 Cracking patterns in CSCBD specimens with different crack lengths for: ψ=75°; (a) 2b=10 mm; (b) 2b=20; (c) 2b=30 mm; (d) 2b=40 mm; (e) 2b=50 mm; (f) 2b=60 mm

direction of maximum compressive load. These wing cracks initiating from the tips of the pre-existing central cracks for all crack lengths lesser than 2b=50 mm, for the crack inclination angle, ψ=45° and 2b=30 mm and also for the crack inclination angle, ψ=75°. As it is clearly evident from Figs. 5(f) and 6(d)-(f), the wing cracks may not initiate from the tips of the pre-existing single crack when the crack length are close to 2b=50 mm for ψ=45°, and 2b=30 mm and ψ=75°, respectively. Alternatively, the specimens can break away due to the indirect tensile effect (axial splitting) exactly like those of the un-cracked Brazilian disc specimens in conventional Brazilian test. It is clearly evident from Figs. 5(f) and 6(d)-(f), that the cracks may not propagate from the tips but propagating from the side-walls, therefore crack initiation mechanism can't be analyzed using fracture mechanics theory (limitation of LEFM). The Linear and non-linear fracture mechanics principles use the stress intensity factors at the tips of the pre-existing cracks/notches/flaws for crack analyses. The experimental conditions shown in these Figs. illustrate that there is no singularity in the problem and the classical theory of elasticity is quite sufficient to solve the boundary value problem by computing the induced stress which may cause the specimen failure. Alternatively, when the tensile stress concentration induced in the side-walls reaches to that of the concrete tensile strength, the crack may be initiated from the these points due to axial splitting phenomena which is more common in ordinary indirect tensile strength tests.

4. Numerical simulations of CSCBD specimens

In this study, the Displacement Discontinuity Method (DDM) originally proposed by Crouch (1967a) for the solution of elasto-static problems in solid mechanics is modified to simulate the CSCBD specimens (Scavia 1990).

4.1 Higher order displacement discontinuity method (HDDM)

Higher accuracies of the normal and shear displacement discontinuities along the boundary of the problem can be obtained by using cubic displacement discontinuity (DD) elements. A cubic variation of DD elements can also be used which divide each boundary element into four equal sub-elements. Either of these sub-elements may contain a central node where the nodal DD is numerically evaluated (Haeri 2015a).

Considering a cubic variation of the displacement discontinuity function, $D_k(\varepsilon)$ (as shown in Fig. 6), the function, $D_k(\varepsilon)$ gives the variation of displacement discontinuities along a line crack and can be used to calculate two fundamental variables of each element (the opening displacement discontinuity D_y and sliding displacement discontinuity D_x) (Haeri 2015a).

$$D_k(\varepsilon) = \sum_{i=1}^{4} \Pi_i(\varepsilon) D_k^i, \quad k = x,y \tag{4}$$

Where $D^1{}_k$ (i.e., $D^1{}_x$ and $D^1{}_y$, $D^2{}_k$(i.e., $D^2{}_x$ and $D^2{}_y$, $D^3{}_k$ (i.e., $D^3{}_x$ and $D^3{}_y$) and $D^4{}_k$(i.e., $D^4{}_x$ and $D^4{}_y$) are the cubic nodal displacement discontinuities and

$$\Pi_1(\varepsilon) = -\left(3a_1^3 - a_1^2\varepsilon - 3a_1\varepsilon^2 + \varepsilon^3\right) \Big/ \left(48a_1^3\right),$$
$$\Pi_2(\varepsilon) = \left(9a_1^3 - 9a_1^2\varepsilon - a_1\varepsilon^2 - \varepsilon^3\right) \Big/ \left(16a_1^3\right),$$
$$\Pi_3(\varepsilon) = \left(9a_1^3 + 9a_1^2\varepsilon - a_1\varepsilon^2 - \varepsilon^3\right) \Big/ \left(16a_1^3\right),$$

$$\Pi_4(\varepsilon) = -\left(3a_1^3 + a_1^2\varepsilon - 3a_1\varepsilon^2 - \varepsilon^3\right)/\left(48a_1^3\right) \tag{5}$$

are the cubic collocation shape functions using a_1=a_2=a_3=a_4. As shown in Fig. 7, a cubic displacement discontinuity (DD) element is divided into four equal sub-elements (each sub-element contains a central node for which the nodal displacement discontinuities are evaluated numerically).

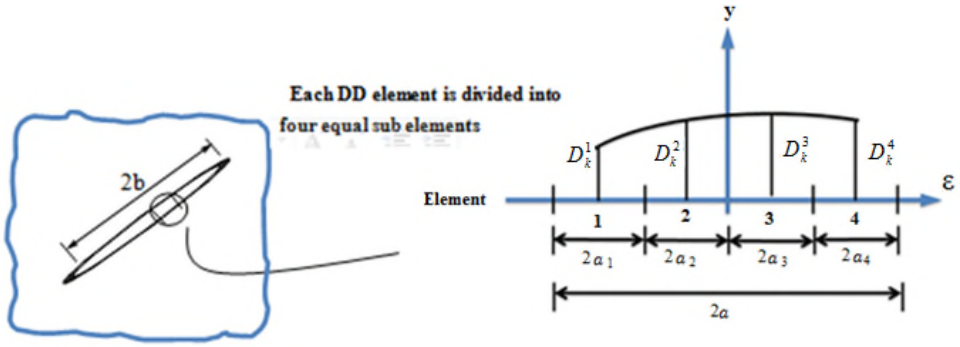

Fig. 7 Cubic shape function showing the variation of higher order displacement discontinuities along an ordinary boundary element

The potential functions $f(x,y)$, and $g(x,y)$ for the cubic case can be find from

$$\begin{aligned} f(x,y) &= \frac{-1}{4\pi(1-\nu)}\sum_{i=1}^{4} D_x^i F_i(I_0, I_1, I_2, I_3) \\ g(x,y) &= \frac{-1}{4\pi(1-\nu)}\sum_{i=1}^{4} D_y^i F_i(I_0, I_1, I_2, I_3) \end{aligned} \tag{6}$$

in which the common function F_i, is defined as

$$F_i(I_0, I_1, I_2, I_3) = \int \Pi_i(\varepsilon) \ln\left[(x-\varepsilon) + y^2\right]^{\frac{1}{2}} d\varepsilon, \quad \text{i} = 1, \text{to } 4 \tag{7}$$

where the integrals I0, I1 , I2 and I3 are expressed as follows

The singularities of the stresses and displacements near the crack ends may reduce their accuracies, special crack tip elements can be effectively used to increase the accuracy of the DDs near the crack tips. As shown in Fig. 8, the DD variations for three nodes can be formulated using

$$I_0(x,y) = \int_{-a}^{a} \ln\left[(x-\varepsilon)^2 + y^2\right]^{\frac{1}{2}} d\varepsilon,$$

$$I_1(x,y) = \int_{-a}^{a} \varepsilon \ln\left[(x-\varepsilon)^2 + y^2\right]^{\frac{1}{2}} d\varepsilon,$$

$$I_2(x,y)=\int_{-a}^{a}\varepsilon^2\ln\left[(x-\varepsilon)^2+y^2\right]^{\frac{1}{2}}d\varepsilon,$$
$$I_3(x,y)=\int_{-a}^{a}\varepsilon^3\ln\left[(x-\varepsilon)^2+y^2\right]^{\frac{1}{2}}d\varepsilon \tag{8}$$

a special crack tip element containing three nodes (or having three special crack tip sub-elements).

$$D_k(\varepsilon)=[\Gamma_{C1}(\varepsilon)]D_k^1(a)+[\Gamma_{C2}(\varepsilon)]D_k^2(a)+[\Gamma_{C3}(\varepsilon)]D_k^3(a),\quad k=x,y \tag{9}$$

where, each crack tip element has a length $a_1=a_2=a_3$. Considering a crack tip element with the three equal sub-elements ($a_1=a_2=a_3$), the shape functions $\Gamma_{C1}(\varepsilon)$, $\Gamma_{C2}(\varepsilon)$ and $\Gamma_{C3}(\varepsilon)$ can be obtained as

$$\Gamma_{C1}(\varepsilon)=\frac{15\varepsilon^{\frac{1}{2}}}{8a_1^{\frac{1}{2}}}-\frac{\varepsilon^{\frac{3}{2}}}{a_1^{\frac{3}{2}}}+\frac{\varepsilon^{\frac{5}{2}}}{8a_1^{\frac{5}{2}}},$$
$$\Gamma_{C2}(\varepsilon)=\frac{-5\varepsilon^{\frac{1}{2}}}{8a_1^{\frac{1}{2}}}+\frac{3\varepsilon^{\frac{3}{2}}}{2\sqrt{3}a_1^{\frac{3}{2}}}-\frac{\varepsilon^{\frac{5}{2}}}{4\sqrt{3}a_1^{\frac{5}{2}}}, \tag{10}$$
$$\Gamma_{C3}(\varepsilon)=\frac{3\varepsilon^{\frac{1}{2}}}{8\sqrt{5}a_1^{\frac{1}{2}}}-\frac{\varepsilon^{\frac{3}{2}}}{2\sqrt{5}a_1^{\frac{3}{2}}}+\frac{\delta^{\frac{5}{2}}}{8\sqrt{5}a_1^{\frac{5}{2}}}$$

Based on the linear elastic fracture mechanics (LEFM) principles, the Mode I and Mode II stress intensity factors KI and KII, (expressed in MPa m1/2) can be written in terms of the normal and shear displacement discontinuities (Shou and Crouch 1995) obtained for the last special crack tip element as

$$K_I=\frac{\mu}{4(1-\nu)}\left(\frac{2\pi}{a_1}\right)^{\frac{1}{2}}D_y(a_1),\quad \text{and}\quad K_{II}=\frac{\mu}{4(1-\nu)}\left(\frac{2\pi}{a_1}\right)^{\frac{1}{2}}D_x(a_1) \tag{11}$$

where, μ is the shear modulus and ν is Poisson's ratio of the brittle material.

4.2 Effects of number of elements and the ratio of crack tip element length, L to the half crack length, b (L/b ratio)

Effects of the number of elements and the ratio of crack tip elements, L to the half crack length, b (L/b ratio) on the values of the normalized Mode I and Mode II stress intensity factors for the numerically simulated CSCBD specimens (with 45 degrees center slant crack i.e., ψ=45°) are investigated by the proposed boundary element method.

The normalized Mode I and Mode II SIFs are simplified as

$$K_I^N = K_I \Big/ \frac{F\sqrt{b}}{\sqrt{\pi}RB}$$
$$K_{II}^N = K_{II} \Big/ \frac{F\sqrt{b}}{\sqrt{\pi}RB} \tag{12}$$

The normalized stress intensity factors $K^N{}_1$ and $K^N{}_{II}$ are 0.721 and1.014, respectively, for this problem i.e., ($K^N{}_1$=0.721 and $K^N{}_{II}$ =1.014). Effect of different number of elements along the crack on normalized SIFs, ($K^N{}_1$and $K^N{}_{II}$), for ψ= 45° is shown in Fig. 9. The figure illustrates the high accuracy of the proposed boundary element method by using a relatively small number of elements (about 6 cubic displacement discontinuity elements containing twenty four nodes).

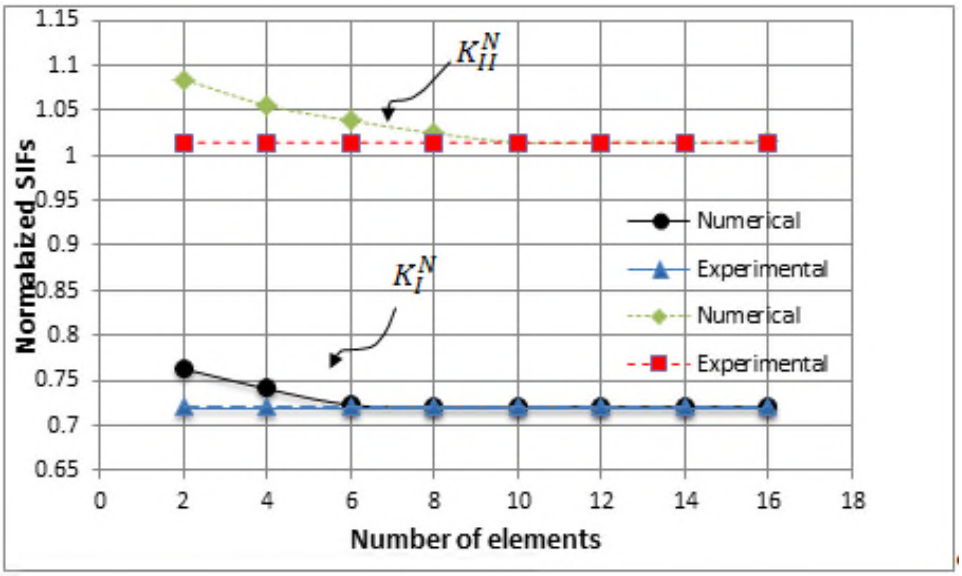

Fig. 9 The normalized SIFs ($K^N{}_1$ and $K^N{}_{II}$), for the 45 degrees center crack (ψ= 45°), using different number of elements and a constant L/b=0.2

Effect of the ratio of crack tip element length, L to the half crack length, b (L/b ratio), for ψ=45° is shown in Fig. 10. As shown in this figure, the L/b ratios between 0.075 and 0.25 give accurate results and throughout this text a constant L/b ratio equal to 0.2 has been used.

In the numerical analysis of the present problem, 6 cubic elements (6 cubic elements containing twenty four sub-elements or nodes) along the pre-existing crack, three special crack tip elements, and L/b=0.2 are used.

4.3 Numerical simulation of CSCBD specimens

In this study, the modified higher order DDM is used to numerically simulate the CSCBD

specimens (prepared from concrete-like materials) under compressive line loading.

Cubic elements formulation of two dimensional DDs along with three special crack tip elements is used to develop a computer code for the solution of plane elasticity crack problems. This method more efficiently improves the accuracy of the conventional DD method. However, using three special elements for the treatment of each crack tip is somewhat complicated but it will greatly increase the accuracy of the DD variations near these singular ends.

The LEFM principles are used to calculate the Mode I and Mode II stress intensity factors (SIFs)) and σ-criterion is also implemented for predicting the wing cracks initiation. In this computer code, the cubic DD elements (i.e., using relatively smaller number of elements but larger number of nodes) give accurate results for the Mode I and Mode II stress intensity factors.

The mechanical properties (i.e., input parameters) of the simulated specimens are the same as those already given in experimental works (Table 1). In the simulation of the cracked discs specimens, the discretization of the cracking boundaries have been accomplished by using 14 cubic elements along Brazilian discs and 10 cubic elements along each central crack. In addition, in the propagation process of the cracks, the crack propagation angle θ for each crack has been calculated in different steps by incrementally extending crack length in the direction of θ for about 1-2 mm in each step. Two cubic elements are taken along each crack increment and three crack tip elements are also added to the last crack increment. In the numerical modeling, the ratio of crack tip length, L to the crack length, b is 0.2 (L/b =0.2) and three special crack tip elements are used. The experimental works are carried out in three-dimension but the numerical analyses are done in two dimensions assuming plain strain condition. The thickness of the specimen (third dimension of the crack) is 30 mm which is 3 times more than that of the crack length (for $2b$=10 mm). For most of the cases the plain strain condition is imposed. In the computer code the plain strain condition is always used as a default because in the classical fracture mechanics the fracture toughness KIC is based on this condition. Therefore, in most of the analyses it is tried to be very close to the plain strain conditions.

The numerical results are compared with the corresponding experimental results obtained in the previous sections of this research. These comparisons give a better knowledge of the crack propagation mechanism and breaking of the brittle materials such as concrete specimens

Table 2 shows a comparison of the numerical and experimental results considering the wing cracks initiation loads.

Effects of the specimen boundary on the crack propagation mechanism of the CSCBD

Table 2 Comparing the wing crack initiation loads (using the proposed code and experiments)

	wing crack initiation loads (KN)			
	Experimental		Numerical	
b/R ratios	Crack inclination angle (ψ)			
	ψ=45°	ψ=75°	ψ=45°	ψ=75°
0.1	2.8	5.8	3	6
0.2	2.3	5.1	2.2	5.3
0.3	1.9	4.4	2	4.5
0.4	1.7	3.6	1.8	3.7
0.5	1.5	2.9	1.7	2.8
0.6	1.4	2.7	1.5	2.9

Table 3 The experimental and numerical values of K_I and K_{II} for different crack lengths (for two cases, ψ=45° and ψ=75°)

b/R ratios	Mode I and Mode II stress intensity factors, K_I and K_{II} (MPa m1/2),							
	Experimental				Numerical			
	ψ=45°		ψ=75°		ψ=45°		ψ=75°	
	K_I	K_{II}	K_I	K_{II}	K_I	K_{II}	K_I	K_{II}
0.1	-0.0759	0.1481	-0.4172	0.1508	-0.0753	0.1487	-0.4185	0.1513
0.2	-0.0934	0.1695	-0.5031	0.1746	-0.0948	0.1691	-0.5042	0.1741
0.3	-0.1032	0.1671	-0.5268	0.1693	-0.1023	0.1678	-0.5245	0.1713
0.4	-0.1193	0.1663	-	-	-0.1206	0.1669	-	-
0.5	-0.1338	0.1561	-	-	-0.1362	0.1569	-	-
0.6	-	-	-	-	-	-	-	-

specimen containing a central straight through crack are studied using proposed code by choosing ψ angles as 45 and 75 degrees. The Mode I and Mode II stress intensity factors, (K_I and K_{II}), for different *b/R* ratios for two case ψ=45° and ψ=75° (which can be estimated experimentally from Eq.s (1)) are evaluated numerically by means of the higher order displacement discontinuity method. The ratios of b to R are taken as *b/R*=0.1,0.2,0.3,0.4,0.5,0.6.

According to the results presented in Table 3, for CSCBD specimens with crack inclination angle, ψ=45°, it can be concluded that with enhancing the *b/R* ratio more than about 0.1, the value $|K_I|$ also increase sharply. In the case of K_{II} value, this value increases when the *b/R* ratio is 0.1<*b/R*<0.2 and decrease is *b/R* > 0.2.

For CSCBD specimens with crack inclination angle, ψ=75°, it can be concluded that the $|K_I|$ value increases from *b/R*=0.1 to 0.3 and decreases from *b/R*=0.3 to *b/R*=0.6, but, the K_{II} value increases when the *b/R* ratio is 0.1<*b/R*<0.2 and decrease is *b/R*> 0.2.

Eq. (1) is given by Atkinson for estimating the fracture toughness of brittle solids (Atkinson *et al*. 1982, Whittaker *et al*. 1992). The Atkinson's formula is used for experimental work and the numerical results are compared with the experimental results estimated from Atkinson's formula. As shown in Table 3 the proposed numerical method gives very accurate results for CSCBD specimens. Thus this method may be considered as a suitable tool for the analysis of cracks propagation and breakage process in brittle materials.

The HDDM method using cubic elements have reached to the experimental results (estimated experimentally from Eq. (1)) when using relatively smaller number of elements (about 6 cubic elements containing twenty four sub-elements or having twenty four nodes) along the crack. The effect of *L/b* ratio on the results given by the proposed method is also noticeable. Although the results obtained by the proposed method, the *L/b* ratios between 0.075 and 0.25 give accurate results and are in good agreement with the experimental results (estimated experimentally from Eq. (1)).

5. Discussions and conclusions

The fracture propagation mechanism of brittle solids such as concrete structures under various loading conditions can be important in studying the fracture mechanics. In this study, a

simultaneous numerical-experimental analysis of crack propagation process in the central Straight through Crack Brazilian Disc (CSCBD) specimens has been accomplished the Mode I and Mode II stress intensity factors (SIFs), K_I and K_{II}, for the pre-existing cracks and propagating wing cracks have been estimated both by numerical simulation. Numerical simulations are done using the Higher order Displacement Discontinuity Method (HDDM) based on SIF concepts of Linear Elastic Fracture Mechanics (LEFM).

Effects of crack lengths on the fracturing process of the concrete-like CSCBD specimens have been discussed. It has been shown that the breaking of concrete-like CSCBD specimens occur mainly by the propagation of wing cracks emanating from the tips of the pre-existing cracks.
In this study, it has been clearly demonstrated that the corresponding numerical results are in good agreement with the experimental results which enables one to clearly understand the fracturing mechanism of pre-cracked concrete like materials (brittle solids).

It is well shown that by comparing the two different crack inclinations (ψ=45° and 75°), the effect of crack lengths shows that the Mode I and Mode II stress intensity factors, K_I and K_{II}, have a strong influence on the final specimen's fracturing path. For a detailed study, the numerical results of cracks initiation stresses and K_I and K_{II} are also compared with the corresponding experimental results for various cases and shown in Tables 2 and 3.

It is expected that the numerical and experimental results presented in this research may improve the understanding of the mechanisms of fracturing and cracks coalescence in the pre-cracked brittle solids such as concrete structures and can also be useful to analyze the stability of rock structures, such as surface and underground mines, tunnels, rock slopes. Furthermore, this approach can be extended and used to study the fracturing mechanism of brittle materials under various loading conditions (e.g., triaxial compressive, tensile and shear loading conditions).

References

Al-Shayea, N.A. (2005), "Crack propagation trajectories for rocks under mixed mode I-II fracture", *Eng. Geol.*, **81**(1), 84-97.

Atkinson, C., Smelser, R.E. and Sanchez, J. (1982), "Combined mode fracture via the cracked Brazilian disk", *Int. J. Fract.*, **18**(4), 279-291.

Ayatollahi, M.R. and Aliha, M.R.M. (2008), "On the use of Brazilian disc specimen for calculating mixed mode I-II fracture toughness of rock materials", *Eng. Fract. Mech.*, **75**(16), 4631-4641.

Ayatollahi, M.R. and Sistaninia, M. (2011), "Mode II fracture study of rocks using Brazilian disk specimens", *Int. J. Rock Mech. Min.*, **48**(5), 819-826.

Bieniawski, Z.T. (1967), "Mechanism of brittle fracture of rock part II-experimental studies", *Int. J. Rock Mech. Min.*, **4**(4) 407-423.

Chen, J.T. and Hong, H.K. (1999), "Review of dual boundary element methods with emphasis on hyper singular integrals and divergent series", *Appl. Mech. Rev.*, **52**(1), 17-33.

Cheng-zhi, P. and Ping, C. (2012), "Breakage characteristics and its influencing factors of rock-like material with multi-fissures under uniaxial compression", *Tran. Nonferrous Met. Soc. China*, **22**(1), 185-191.

Crouch, S.L. (1967), "Analysis of stresses and displacements around underground excavations: an application of the displacement discontinuity method", University of Minnesota Geomechanics Report, Minneapolis, Minnesota.

Dai, F. Chen, R, Iqbal, M.J. and Xia, K. (2010), "Dynamic cracked chevron notched Brazilian disc method for measuring rock fracture parameters", *Int. J. Rock Mech. Min.*, **47**(4), 606-613.

Dai, F., Xia, K., Zheng, H. and Wang, Y.X. (2011), "Determination of dynamic rock mode-I fracture parameters using cracked chevron notched semi-circular bend specimen", *Eng. Fract. Mech.*, **78**, 2633-

2644.
Haeri, H. (2015a), *Coupled experimental-numerical fracture mechanics*, Lambert Academic Press, Germany.
Haeri, H. (2015b), "Influence of the inclined edge notches on the shear-fracture behavior in edge-notched beam specimens", *Comput. Concrete*, **16**(4), 605-623.
Haeri, H. (2015c), "Simulating the crack propagation mechanism of pre-cracked rock like shear specimens", *Strength. Mater.*, **47**(4), 618-632.
Hoek, E. and Bieniawski, Z.T. (1965), "Brittle rock fracture propagation in rock under compression, South African council for scientific and industrial research pretoria. *Int. J. Frac. Mech.* **1**(3), 137-155.
Ingraffea, A.R. (1985), "Fracture Propagation in Rock", *Mech. Geomater.* 219-258.
Irwin, G.R. (1957), "Analysis of stress and strains near the end of a crack", *J. Appl. Mech.*, **24**, 361.
Janeiro, R.P and Einstein, H.H. (2010), "Experimental study of the cracking behavior of specimens containing inclusions (under uniaxial compression)", *Int. J. Fract.* **164**, 83-102.
Ke, C.C, Chen, C.S and Tu, C.H (2008), "Determination of fracture toughness of anisotropic rocks by boundary element method", *Rock Mech. Rock Eng.*, **41**(4), 509-538.
Lee, H. and Jeon, S. (2011), "An experimental and numerical study of fracture coalescence in pre-cracked specimens under uniaxial compression", *Int. J. Solid. Struct.*, **48**(6), 979-999.
Natarajana, S., Mahapatrab, D.R. and Bordas, S.P.A. (2010), "Integrating strong and weak discontinuities without integration subcells and example applications in an XFEM/GFEM framework", *Int. J. Numer Meth. Eng.*, **83**, 269-294.
Park, C.H. and Bobet, A. (2010), "Crack initiation, propagation and coalescence from frictional flaws in uniaxial compression", *Eng. Fract. Mech.*, **77**(14), 2727-2748.
Ravi-Chandar, K. and Knauss, W.G. (1984), "An experimental investigation into dynamic fracture: III. On steady-state crack propagation and crack branching", *Int. J. Fract.* **26**(2), 141-154.
Scavia, C. (1990), "Fracture mechanics approach to stability analysis of crack slopes", *Eng. Fract. Mech.*, **35**(4), 889-910.
Shen, B., Stephansson, O., Einstein, H.H. and Ghahreman, B. (1995), "Coalescence of fractures under shear stress experiments", *J. Geophys. Res.*, **100**(B4), 5975-5990.
Shou, K.J. and Crouch, S.L. (1995), "A higher order displacement discontinuity method for analysis of crack problems", *Int. J. Rock Mech. Min. Sci. Geomech.*, **32**(1), 49-55.
Wallin, K. (2013), "A simple fracture mechanical interpretation of size effects in concrete fracture toughness tests", *Eng. Fract. Mech.*, **99**, 18-29.
Wang, Q.Z (2010), "Formula for calculating the critical stress intensity factor in rock fracture toughness tests using cracked chevron notched Brazilian disc (CCNBD) specimens", *Int. J. Rock Mech. Min. Sci.*, **47**(6), 1006-1011.
Wang, Q.Z., Feng, F., Ni, M. and Gou, X.P. (2011), "Measurement of mode I and mode II rock dynamic fracture toughness with cracked straight through flattened Brazilian disc impacted by split Hopkinson pressure bar", *Eng. Fract. Mech.*, **78**(12), 2455-2469.
Wang, Q.Z., Gou, X.P. and Fan, H. (2012), "The minimum dimensionless stress intensity factor and its upper bound for CCNBD fracture toughness specimen analyzed with straight through crack assumption", *Eng. Fract. Mech.*, **82**, 1-8.
Whittaker, B.N., Singh, R.N. and Sun, G. (1992), *Rock fracture mechanics principles, design and applications, developments in geotechnical engineering*, Elsevier, Amsterdam.
Yang, Q., Dai, Y.H., Han, L.J. and Jin, Z.Q. (2009), "Experimental study on mechanical behavior of brittle marble samples containing different flaws under uniaxial compression", *Eng. Fract. Mech.*, **76**(12), 1833-1845.
Yang, S.Q (2011), "Crack coalescence behavior of brittle sandstone samples containing two coplanar fissures in the process of deformation breakage", *Eng. Fract. Mech.*, **78**(17), 3059-3081.